Semiconductor Physics, Quantum Electronics & Optoelectronics, 2025. V. 28, No 3. P. 306-314.

Hetero- and low-dimensional structures

MXene-integrated two-dimensional photocatalysts: A new frontier in sustainable degradation of organic dyes

J.A. Buledi[1,2], S. Golovynskyi[2], V.M. Kravchenko[3], J. Qu[2], I. Golovynska[2,*], A.R. Solangi[1]

[1]*National Centre of Excellence in Analytical Chemistry, University of Sindh, 76080 Jamshoro, Pakistan*
[2]*College of Physics and Optoelectronic Engineering, Shenzhen University, 518060 Shenzhen, Guangdong, P.R. China*
[3]*Taras Shevchenko National University of Kyiv, Physics Faculty, 01601 Kyiv, Ukraine*
[*]*Corresponding author e-mail: iuliia@szu.edu.cn*

Abstract. MXene-based two-dimensional (2D) composites, a class of graphene-like transition metal carbides and nitrides, are emerging as excellent materials for photocatalytic applications due to their promising characteristics, including tunable functionalities and a large surface area. To fabricate MXene-based photocatalysts, various synthesis routes are used, namely, hydrothermal, solvothermal, electrostatic self-assembly, and chemical vapor deposition. The solvothermal and hydrothermal synthesis methods enhance crystallinity and accelerate charge transfer, preventing recombination and boosting photocatalytic activity. Furthermore, etching methods influence MXene's physicochemical properties, impacting pollutant removal efficiency. MXene composites are used as promising photocatalysts to degrade organic dyes, including Congo Red, Methylene Orange, Rhodamine B, and Methylene Blue. MXene composites, namely TiO_2/Ti_3C_2, Bi_2WO_6/Nb_2CT_x and MXene/g-C_3N_4, demonstrate excellent photocatalytic performance, achieving over 90% degradation rate under visible irradiation. However, challenges such as scalability, energy consumption, and structural stability need further investigation to optimize their large-scale applications.

Keywords: MXene composites, 2D nanocomposites, environmental remediation, organic contaminants, environmental pollution.

https://doi.org/10.15407/spqeo28.03.306
PACS 73.61.Ey, 81.16.Hc, 82.50.-m, 85.35.Be, 92.40.kc, 92.40.qc

Manuscript received 12.05.25; revised version received 20.07.25; accepted for publication 03.09.25; published online 24.09.25.

1. Introduction

Urbanization, industrialization, and rapid infrastructure development have increased environmental challenges worldwide [1, 2]. Among the major contributors to environmental contamination, industrial waste poses important risks due to inappropriate disposal and inadequate wastewater treatment. Discharging untreated industrial runoffs severely pollutes natural ecosystems, causing harm to human health and the aquatic system. Several industries, including printing, textiles, agriculture, polymer production, and nuclear sectors, discharge harmful pollutants, namely azo dyes, pesticides, and toxic chemicals, which damage freshwater resources and disrupt aquatic biodiversity [3, 4]. Knowing these environmental threats, international organizations like the Environmental Protection Agency and World Health Organization have imposed strict regulations, compelling industries to incorporate effective wastewater treatment solutions [5]. To tackle Industrial water pollution, several wastewater treatment methods were developed, namely adsorption [6], precipitation [7], biodegradation [8], solvent extraction [9], membrane separation [10], chlorination, and sonodegradation [11]. Nevertheless, these conventional methods often have limitations, *e.g.*, incomplete pollutant removal, high operational costs, and secondary pollution. Among these advanced treatment methods, photocatalysis gains considerable attention due to its high performance, eco-friendliness, cost-effectiveness, and ability to fully degrade pollutants into non-toxic byproducts [12].

Photocatalytic degradation, in particular, employs solar light to break down pollutants, making it an energy-efficient and sustainable solution for wastewater treatment. This technique presents an effective pathway toward enduring environmental remediation and Industrial sustainability [13]. Photocatalysis is a promising process for removing pollutants from water using a photocatalyst under UV-visible light [14]. This method creates electron-hole pairs (e-h), where holes initiate oxidation, and electrons drive reduction reactions, breaking down pollutants [15]. Different photocatalytic materials are employed, namely molybdenum disulfide (MoS_2) [16], tungsten disulfide (WS_2) [17], cerium oxide (CeO_2) [18], and titanium dioxide (TiO_2) [19]. However, many of these materials

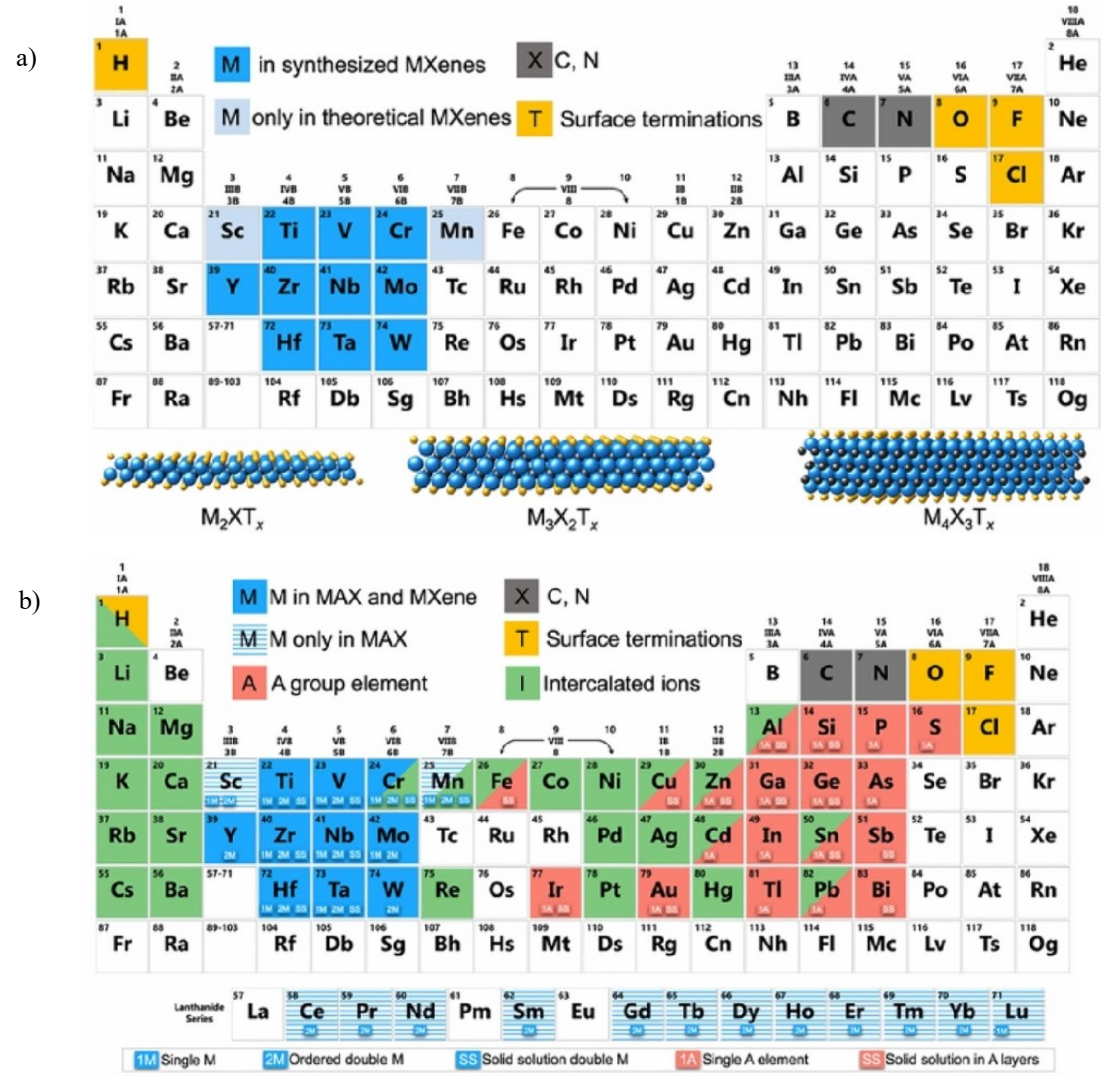

Fig. 1. Elemental map showing the composition of MXenes and MAX phases. (a) The elements used for the synthesis of MXenes (bright blue) and those experimentally not confirmed (light blue); the three typical MXene structures are shown at the bottom. (b) Elements used for the synthesis of MXenes, MAX phases, and their intercalated ions. Reprinted with permission from Ref. [24]. Copyright 2019, American Chemical Society.

suffer from poor charge separation, limited light absorption, and low stability, which limits their effectiveness in wastewater treatment. To overcome these restrictions, researchers must develop advanced photocatalytic materials with enhanced proficiency, improved stability, and broad-spectrum absorption for sustainable environmental remediation [20]. MXene was first discovered as a photocatalyst in 2014, and, since then, several studies have highlighted its potential for degrading toxic environmental pollutants in water [21]. MXenes ($M_{n+1}X_nT_x$) are compounds of early transitional metal atoms (M = Ti, Nb, Mo, *etc.*) with nonmetal atoms (X = C, N) and surface terminations (T_X = O, OH, F, Cl) [22, 23]. MXenes are a rapidly expanding class of two-dimensional (2D) materials that originate from transition metal carbides and nitrides. These materials comprise layered structures, where $n + 1$ layers of early transition metals (M, shown in blue in Fig. 1) alternate with n layers of carbon or nitrogen (X, depicted in gray in Fig. 1).

The elements with a stripped blue background show that these have been used in MAX phases, and their MXenes have not been prepared yet. Elements in the red background are the A elements that can be selectively etched to build MXenes. The green background elements are cations that have been intercalated into MXenes. The 1M and 1A indicate the possibility for the formation of single pure transition metal and A element MXenes. SS shows the solid solution in the transition metal atomic planes (blue) or A element planes (red). 2M shows the possibility for the formation of a double transition metal MAX phase or MXene.

Their general formula is $M_{n+1}X_nT_x$, where T_x represents surface terminations, namely –O, –OH, –F, and/or –Cl (marked in orange in Fig. 1). The structural diversity of MXenes, illustrated at the bottom of Fig. 1a, contributes to their versatility in numerous applications. Moreover, MXenes (Fig. 1a), their precursor MAX phases, and intercalated metal ions (Fig. 1b) exemplify

fundamental chemical principles, demonstrating how elemental building blocks can be manipulated to develop innovative nanomaterials [24]. MXenes demonstrate a large specific surface area, exceptional electrical conductivity, and tunable band gaps (0.05–2.87 eV), making them superior to other 2D materials in photocatalysis [25]. Compared to graphene-based photocatalysts, MXene-based ones demonstrate somewhat higher photocatalytic efficiency. For instance, Ti_3C_2/MoS_2 achieves 97.4% dye degradation, surpassing g-C_3N_4/Ag/GO (78%) [26]. This is attributed to MXene's unique functional groups (–F, –OH) and strong electrostatic interactions [27].

This mini-review examines MXene's role in organic pollutant degradation. It also discusses its different synthesis techniques and future challenges for enhancing MXene-based photocatalysis.

2. Different synthesis methods for the fabrication of MXene composites

Various methods are employed to synthesize MXene-based photocatalysts, including electrostatic self-assembly, hydrothermal and solvothermal treatments, calcination, mechanical/ultrasonic mixing, and others [28]. Generally, MXene is synthesized from its parent material, Ti_3AlC_2. This process is usually completed by removing the Al layer from the parent material. Moreover, the HF acid method was the first to eliminate the Al layer from the parent material. The details of producing MXene from the MAX (M is an early transition metal, A is an A-group element, and X is either C and/or N) phase are described in reactions 1, 2, and 3. In addition, the generation of –F and –OH groups are highlighted in the second and third steps of the reactions.

$$Ti_3AlC_2 + 3HF \rightarrow AlF_3 + 3/2\,H_2 + Ti_3C_2. \quad (1)$$

$$Ti_3C_2 + 2H_2O \rightarrow Ti_3C_2(OH)_2 + H_2. \quad (2)$$

$$Ti_3C_2 + 2HF \rightarrow Ti_3C_2F_2 + H_2. \quad (3)$$

Among all reported methods, mechanical/ultrasonic mixing is the simplest. This method involves vigorous mechanical stirring or high-intensity ultrasonic vibrations, ensuring strong interactions between MXenes and photocatalysts. For instance, $Ti_3C_2T_x$ hydrogels are synthesized by stirring MXenes and graphene oxide colloidal solutions with Eosin Y, followed by heating at 70 °C under N protection. Additionally, CdS/MXene (Ti_3C_2) composites are fabricated using electrostatic self-assembly, where CdS nanowires are uniformly dispersed on MXene nanosheets *via* electrostatic attraction [29].

The hydrothermal and solvothermal processes are also extensively used to obtain MXene-based composites. The solvothermal method is applied in an *in situ* metal-organic-framework-derived approach to developing Co-Co layered double hydroxide/$Ti_3C_2T_x$ nanosheets with excellent photocatalytic properties [30]. Etching techniques are critical for MXene fabrication, utilizing various etchants, namely hydrogen fluoride (HF), lithium fluoride (LiF) with HF, and zinc chloride ($ZnCl_2$). The final MXene properties depend on etchant concentration and etching duration [31]. For instance, the replacement reaction method is used to synthesize Zn-based MAX and Cl-terminated MXenes with $ZnCl_2$ Lewis acidic molten salt, however, challenges, namely high temperatures, crystallinity control, and energy consumption, must be addressed [32]. Additionally, chemical vapor deposition (CVD) techniques are explored for precise MXene film fabrication. 2D ultrathin α-Mo_2C crystals with a large surface area, achieving high-quality, defect-free structures, are successfully synthesized using CVD [33]. Similarly, the one-step copper-catalyzed CVD technique enables the *in situ* synthesis of 2D Mo_2C on graphene. Despite offering high purity and minimal defects, the CVD methods often suffer from low yields and complex processing, highlighting the need for further advancements [34].

3. Application of 2D MXene composites for degradation of organic dyes

3.1. Methylene Orange

Methylene Orange (MO), an organic dye discovered in 1876, was initially recognized for its bicolored nature by Griess [35]. As a sulfonated azo dye, MO is highly stable and non-biodegradable under ambient conditions, posing a significant environmental hazard. It is extensively utilized in industries, namely in food, cosmetics, textiles, leather, pharmaceuticals, and plastics [36]. The large-scale discharge of MO into water bodies disrupts aquatic ecosystems by lowering oxygen levels and hindering photocatalytic degradation. Exposure to MO-contaminated water can lead to respiratory diseases, vomiting, diarrhea, and skin irritation [37]. Different studies are devoted to MO degradation *via* utilizing efficient MXene-based photocatalysts.

Peng *et al.* [38] synthesized a (111) TiO_2/Ti_3C_2 photocatalyst *via* the hydrothermal method to degrade MO dye. Pure TiO_2 had limited photocatalytic efficiency due to a low specific surface area (SSA) and interlayer spacing. However, an incorporated Ti_3C_2 enhanced these properties. This photocatalyst possessed 98.67% MO degradation in 2.3 hours, representing MXene's potential. Moreover, Peng *et al.* [39] synthesized a 2D MXene-based TiO_2/Ti_3C_2 nanocomposite using the hydrothermal partial oxidation method for MO degradation. Transmission electron microscopy and density functional theory confirmed its smooth interface and minimal defects. The photocatalyst achieved 97.4% degradation, with only a 4.9% decline after four cycles, demonstrating excellent recyclability. Jiang *et al*. [40] synthesized a C-TiO_2/Bi_4NbO_8Cl nanocomposite *via* calcination for MO degradation in water and wastewater. Material characterizations confirmed their dissimilar properties. The photocatalyst gained 44% MO degradation in 3 hours, offering a simple approach to designing functional nanomaterials for water purification. Chen *et al*. [41] synthesized a $TiO_2/Ti_3C_2T_x$ nanocomposite using the solvothermal method, with its structure and photocatalytic activity influenced by temperature (333–493 K).

Under a 500 W Hg lamp illumination, it attained 92% MO degradation in 50 min at 473 K, demonstrating efficient charge transfer and enhanced photocatalytic performance for organic pollutant removal.

3.2. Congo Red

According to the literature, Paul Bottiger first discovered Congo Red (CR) in 1885, marking a significant advancement in dye development [42]. CR dyes are widely used in textiles, pharmaceuticals, and the paper industries. However, their presence in industrial effluents affects soil properties and plant health and poses serious risks to human health [43]. In this regard, Iqbal *et al*. [44] synthesized $Bi_{0.9}La_{0.1}FeO_3/Ti_3C_2$ and $Bi_{0.9}La_{0.1}Fe_{0.95}Mn_{0.05}O_3/Ti_3C_2$ photocatalysts using a cost-effective double solvent sol-gel method for efficient CR degradation in water and wastewater. These catalysts exhibited remarkable photodegradation efficiencies of 92% and 93% in the dark within 30 min, attributed to their large specific surface area (39 m^2/g), enhancing active sites and photocatalytic performance. Tariq *et al.* [45] developed a $BiFeO_3/Ti_3C_2$ nanocomposite photocatalyst using the double solvent solvothermal method for efficient CR degradation in water (Fig. 2). The prepared photocatalyst achieved nearly 100% CR removal under visible light irradiation in 2 hours, demonstrating cost-effectiveness and environmental sustainability. Sajid *et al*. [46] synthesized a $BiVO_4/Ti_3C_2$ nanocomposite photocatalyst using a cost-effective hydrothermal method for CR dye degradation. It achieved 99.5% degradation under visible light irradiation in 1 hour. It remained highly efficient after three cycles, making it commercially doable.

3.3. Rhodamine B

Rhodamine B (RhB) is widely used in the cotton industry as a textile dye due to its high durability and resistance to biodegradation. The European Food Safety Authority has classified it as genotoxic and carcinogenic [47]. While nations like China and the EU have banned its use in food [48], it remains prevalent in biotechnology, textiles, and as a water tracer. RhB is one of the most hazardous dyes in wastewater, posing serious risks to human and animal health. Its applications extend to dye lasers, stamp pad inks, and paintings [49]. The following section explores the degradation potential of MXene-based photocatalysts for environmental purification from RhB.

Wu *et al*. [50] employed the one-step *in-situ* calcination method to synthesize a $TiO_2/g–C_3N_4$ photocatalyst from MXene Ti_3C_2 for RhB degradation under visible light irradiation. The photocatalyst achieved 98.0% RhB degradation under a 300 W Xenon lamp illumination in 70 min. Its efficiency surpassed pure TiO_2, g-C_3N_4, and graphene due to its large surface area (26.4 m^2/g) and pore volume (0.135 cm^3/g), which enhanced photon absorption and facilitated photodegradation. The photocatalyst's high surface functionality contributed to its superior performance. Cui *et al*. [51] synthesized ultrathin Bi_2WO_6/Nb_2CT_x hybrid nanosheets *via* the hydrothermal process for RhB photodegradation.

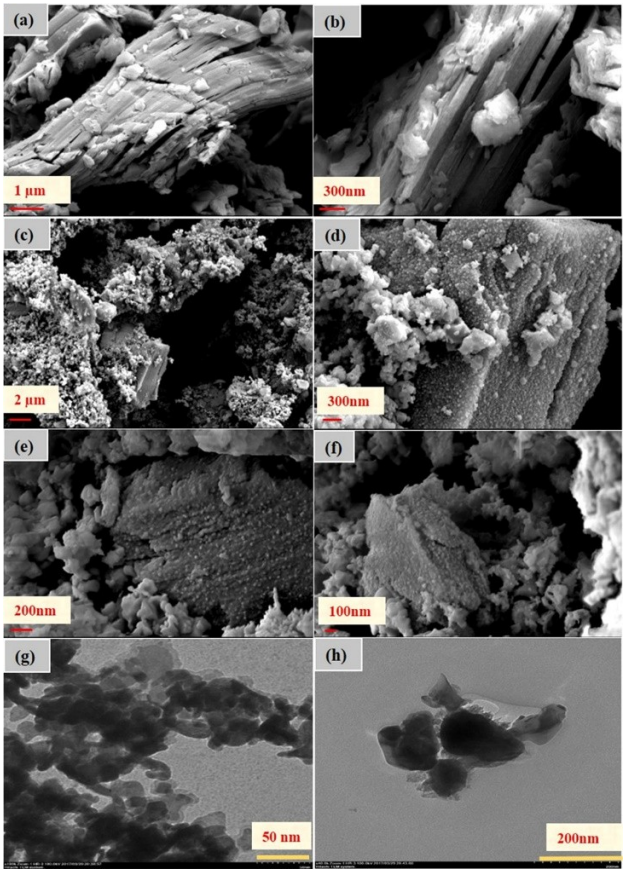

Fig. 2. Nanohybrid system composed of bismuth ferrite nanoparticles $BiFeO_3$ (BFO) with 2D Ti_3C_2 MXene sheets for enhanced photocatalytic activity, fabricated using the double-solvent solvothermal method: (a, b) Exfoliated MXene sheets, (c–f) $BiFeO_3$/MXene nanohybrids, and (g, h) $BiFeO_3$/MXene nanohybrids. Reprinted with permission from Ref. [45]. Copyright 2019, American Chemical Society.

Bi_2WO_6/Nb_2CT_x exhibited superior photocatalytic efficiency of 99.8%, compared to Bi_2WO_6, due to enhanced *e-h* separation, achieving a rate constant of 0.072 min^{-1}, which was 2.8 times higher than that for pure Bi_2WO_6. Ding *et al*. [52] successfully fabricated a 2D $TiO_2@Ti_3C_2/g\text{-}C_3N_4$ photocatalyst by exploiting the ultrasonic-assisted calcination procedure. This method increased the interfacial structure and electronic properties of the prepared material. The active C_3N_4 is involved in *e-h* pair generation, while Ti_3C_2 and TiO_2 facilitate the charge transfer. This synergy effectively boosted the RhB degradation by 1.33 times, respectively. Moreover, Fig. 3 illustrates the charge transfer and *e-h* separation mechanism in $TiO_2@Ti_3C_2/g\text{-}C_3N_4$ used for RhB degradation. Tran *et al.* [53] developed safflower-shaped TiO_2/Ti_3C_2 heterostructures from 2D Ti_3C_2 MXene via hydrothermal, ion exchange, and calcination for RhB photodegradation. The composite reached 95% efficiency in 1 hour due to its porous structure. Characterization techniques confirmed its enhanced photocatalytic activity compared to pure MXene. Diao *et al*. [54] synthesized an efficient $g\text{-}C_3N_4/Ti_3C_2/TiO_2$ photocatalyst *via* CVD and *in situ* growth for RhB degradation. Its uniform structure was

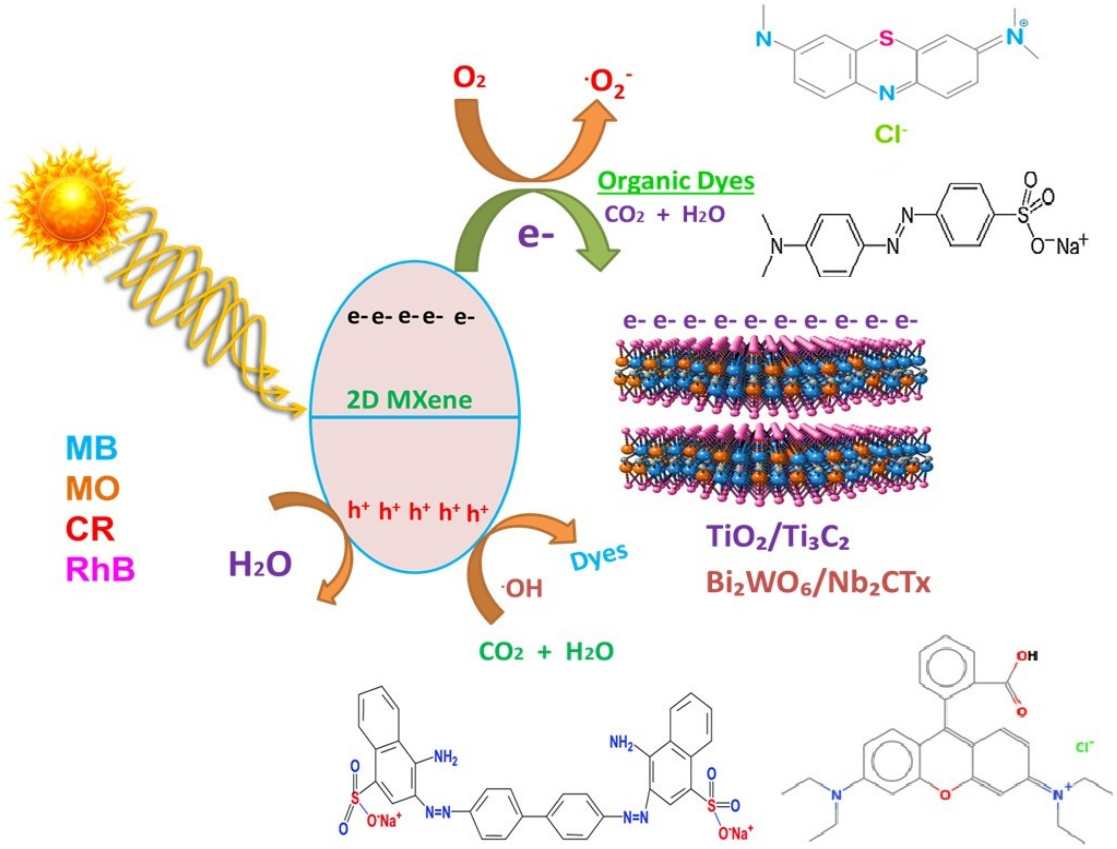

Fig. 3. The proposed degradation mechanism of organic dyes under UV-light irradiation using 2D MXene composites.

demonstrated. The photocatalyst showed 85.1% degradation in 3 hours, achieving three times higher efficiency than pristine materials, with excellent stability and reusability.

3.4. Methylene Blue

Methylene Blue (MB) was first discovered by Caro in 1876 in England [55]. As a phenothiazine compound, its chemical name is tetramethylthionine chloride, appearing deep blue in its oxidized state and colorless when reduced to leuco MB. It dissolves in water and organic solvents and was historically used as an antibacterial and antiseptic dye in medicine [56]. However, MB contamination in water reduces oxygen levels, threatening aquatic life and human health.

Peng *et al*. [38] used a hydrothermal synthesis to fabricate a (111) TiO_2/Ti_3C_2 photocatalyst for MB degradation. Pure TiO_2 exhibited limited photocatalytic efficiency due to low SSA and interlayer spacing, but combining it with Ti_3C_2 improved these properties. The developed photocatalyst showed 85% MB degradation in 2.3 hours, highlighting MXene's potential in advanced photocatalyst design. Cui *et al*. [51] synthesized ultrathin Bi_2WO_6/Nb_2CT_x hybrid nanosheets via the hydrothermal method for RhB, MB, and TC-HCl degradation. Bi_2WO_6 revealed enhanced photocatalytic efficiency when combined with Nb_2CT_X, achieving 92.7% MB degradation. This study highlights Nb_2CT_x as a promising co-catalyst for improved photodegradation performance. In 2022, Qu *et al*. [57] employed HF etching to synthesize an ML-Ti_3C_2 MXene-based photocatalyst from Ti_3AlC_2. The ML-$Ti_3C_2(OH)_2$ photocatalyst demonstrated 81.2% MB degradation within 30 min in the dark due to its high SSA, interlayer spacing, and active sites, offering an efficient method for organic pollutant removal. In 2022, Nasri *et al*. [58] synthesized an MXene/g-C_3N_4 heterostructure photocatalyst using the wet impregnation method. Under a 500 W halogen lamp illumination, the 1 wt.% MXene/g-C_3N_4 photocatalyst showed 69.4% degradation in 3 hours, attributed to enhanced BET SSA, crystallinity, and reduced band gap. The study revealed that electrons played a crucial role in improving photocatalytic performance by preventing charge recombination, thereby increasing activity. This MXene contributed significantly by facilitating charge transfer and segregation, accelerating dye degradation under solar irradiation. In 2022, Liu *et al*. [59] developed a $Ti_3C_2T_x$-derived oxide nanocomposite photocatalyst through prolonged oxidation of $Ti_3C_2T_x$ at a controlled temperature. The synthesized 2D MXene-based photocatalyst exhibited an exceptional MB degradation efficiency of nearly 90% within 1 hour under visible light irradiation. This superior performance was ascribed to its high SSA, increased band gap energy, improved interlayer spacing, and remarkable thermal, optical, and electrical properties. Fig. 3 describes the general mechanism of exploitation of 2D MXenes-based composites for degradation of organic dyes under UV radiation, yielding the final product of H_2O and CO_2.

4. Conclusions and future perspectives

MXene-based nanocomposites emerged as highly efficient photocatalysts for degrading various organic pollutants, including dyes like Methylene Orange (MO), Congo Red (CR), Rhodamine B (RhB), and Methylene Blue (MB). Several fabrication techniques, namely electrostatic self-assembly, hydrothermal and solvothermal synthesis, calcination, and mechanical/ultrasonic mixing, were explored to enhance their photocatalytic efficiency. Among these, the hydrothermal and solvothermal processes demonstrated significant improvements in charge separation and pollutant adsorption. Researchers have successfully integrated MXenes with TiO_2, Bi_2WO_6, and g-C_3N_4, resulting in increased surface area, reduced band gap, and higher electron mobility.

Recent studies have reported remarkable degradation efficiencies, with $Ti_3C_2T_x$-derived nanocomposites achieving up to 98% dye removal under visible light irradiation. Despite these advancements, there are still challenges in large-scale production, stability, and reusability. Future research should focus on optimizing synthesis protocols, enhancing structural stability, and integrating MXenes with plasmonic materials or emerging technologies like AI-driven catalyst design. Additionally, exploring MXene-based heterostructures with multifunctional capabilities can further improve degradation efficiency and sustainability. Advancing MXene photocatalysts for practical waste-water treatment applications will contribute significantly to environmental remediation and sustainable water purification systems, ultimately addressing global pollution challenges through innovative nanomaterial engineering.

Funding and Acknowledgements

This work has been partially supported by the National Natural Science Foundation of China (62127819) and Shenzhen Key Laboratory of Photonics and Biophotonics (ZDSYS20210623092006020).

Declaration of competing interest

The authors declare no competing financial interests or personal relationships to the reported paper.

Data availability

The reported data can be available upon request from the corresponding author.

References

1. Shao L., Chen G. Water footprint assessment for wastewater treatment: method, indicator, and application. *Environ. Sci. Technol.* 2013. **47**. P. 7787–7794. https://doi.org/10.1021/es402013t.
2. Ali H., Ali A., Buledi J.A. *et al*. MXene-based nanocomposites: emerging candidates for the removal of antibiotics, dyes, and heavy metal ions. *Mater. Chem. Front.* 2023. **7**. P. 5519–5544. https://doi.org/10.1039/D3QM00667K.
3. Buledi J.A., Pato A.H., Kanhar A.H. *et al*. Heterogeneous kinetics of CuO nanoflakes in simultaneous decolorization of Eosin Y and Rhodamine B in aqueous media. *Appl. Nanosci.* 2021. **11**. P. 1241–1256. https://doi.org/10.1007/s13204-021-01685-y.
4. Tunesi M.M., Soomro R.A., Han X. *et al*. Application of MXenes in environmental remediation technologies. *Nano Converg.* 2021. **8**. P. 1–19. https://doi.org/10.1186/s40580-021-00255-w.
5. Sheth Y., Dharaskar S., Chaudhary V. *et al*. Prospects of titanium carbide-based MXene in heavy metal ion and radionuclide adsorption for wastewater remediation: A review. *Chemosphere.* 2022. **293**. P. 133563. https://doi.org/10.1016/j.chemosphere.2022.133563.
6. Ahmadpour A. Using of activated carbon adsorption in wastewater industries. *J. Chem. Lett.* 2022. **3**. P. 2–9. https://doi.org/10.22034/JCHEMLETT.2022.334692.1059.
7. Kim J., Yoon S., Choi M. *et al*. Metal ion recovery from electrodialysis-concentrated plating waste-water via pilot-scale sequential electro-winning/chemical precipitation. *J. Clean. Prod.* 2022. **330**. P. 129879. https://doi.org/10.1016/j.jclepro.2021.129879.
8. Liang G., Li S., Yu X. *et al*. Black carbon-mediated degradation of organic pollutants: A critical review. *Process Saf. Environ. Prot.* 2022. **160**. P. 610–619. https://doi.org/10.1016/j.psep.2022.02.049.
9. George A., Raj A.D., Irudayaraj A.A. *et al*. Regeneration study of MB in recycling runs over nickel vanadium oxide by solvent extraction for photocatalytic performance for wastewater treatments. *Environ. Res.* 2022. **211**. P. 112970. https://doi.org/10.1016/j.envres.2022.112970.
10. Kavitha E., Poonguzhali E., Nanditha D. *et al*. Current status and future prospects of membrane separation processes for value recovery from wastewater. *Chemosphere.* 2022. **291**. P. 132690. https://doi.org/10.1016/j.chemosphere.2021.132690.
11. Ileri B., Dogu I. Sono-degradation of Reactive Blue 19 in aqueous solution and synthetic textile industry wastewater by nanoscale zero-valent aluminum. *J. Environ. Manag.* 2022. **303**. P. 114200. https://doi.org/10.1016/j.jenvman.2021.114200.
12. Trojanowicz M., Bojanowska-Czajka A., Bartosiewicz I., Kulisa K. Advanced oxidation/reduction processes treatment for aqueous perfluorooctanoate (PFOA) and perfluorooctanesulfonate (PFOS) – a review of recent advances. *Chem. Eng. J.* 2018. **336**. P. 170–199. https://doi.org/10.1016/j.cej.2017.10.153.
13. Liu X., Chen J., Yang L. *et al*. 2D/2D g-C_3N_4/TiO_2 with exposed (001) facets Z-scheme composites accelerating separation of interfacial charge and visible photocatalytic degradation of Rhodamine B. *J. Phys. Chem. Sol.* 2022. **160**. P. 110339. https://doi.org/10.1016/j.jpcs.2021.110339.
14. Lee S-Y., Park S-J. TiO_2 photocatalyst for water treatment applications. *J. Ind. Eng. Chem.* 2013. **19**. P. 1761–1769. https://doi.org/10.1016/j.jiec.2013.07.012.
15. Belver C., Bedia J., Gómez-Avilés A. *et al*. Semiconductor photocatalysis for water purification. In: *Nanoscale Materials in Water Purification.* 2019. P. 581–651. https://doi.org/10.1016/B978-0-12-813926-4.00028-8.

16. Swain G., Sultana S., Parida K. One-pot-architectured Au-nanodot-promoted $MoS_2/ZnIn_2S_4$: a novel *p-n* heterojunction photocatalyst for enhanced hydrogen production and phenol degradation. *Inorg. Chem.* 2019. **58**. P. 9941–9955. https://doi.org/10.1021/acs.inorgchem.9b01105.
17. Fatima T., Husain S., Narang J. *et al*. Novel tungsten disulfide (WS_2) nanosheets for photocatalytic degradation and electrochemical detection of pharmaceutical pollutants. *J. Water Process Eng.* 2022. **47**. P. 102717. https://doi.org/10.1016/j.jwpe.2022.102717.
18. Mansingh S., Padhi D., Parida K. Enhanced photocatalytic activity of nanostructured Fe doped CeO_2 for hydrogen production under visible light irradiation. *Int. J. Hydrogen Energy.* 2016. **41**. P. 14133–14146. https://doi.org/10.1016/j.ijhydene.2016.05.191.
19. Kitamura Y., Okinaka N., Shibayama T. *et al*. Combustion synthesis of TiO_2 nanoparticles as photocatalyst. *Powder Technol.* 2007. **176**. P. 93–98. https://doi.org/10.1016/j.powtec.2007.02.009.
20. Buledi J.A., Hyder A., Khand N.H. *et al*. Potential mitigation of dyes through mxene composites. In: *Handbook of Functionalized Nanostructured MXenes: Synthetic Strategies and Applications from Energy to Environment Sustainability.* Springer, 2023. P. 283–300.
21. Raheem I., Mubarak N.M., Karri R.R. *et al*. Rapid growth of MXene-based membranes for sustainable environmental pollution remediation. *Chemosphere.* 2023. **311**. P. 137056. https://doi.org/10.1016/j.chemosphere.2022.137056.
22. Gogotsi Y. The future of MXenes. *Chem. Mater*. 2023. **35**. P. 8767–8770. https://doi.org/10.1021/acs.chemmater.3c02491.
23. Tareen A., Khan K., Iqbal M. *et al*. Recent advances in MXenes: new horizons in biomedical technologies. *Mater. Tod. Chem.* 2022. **26**. P. 101205. https://doi.org/10.1016/j.mtchem.2022.101205.
24. Gogotsi Y., Anasori B. The rise of MXenes. In: *MXenes.* Jenny Stanford Publishing, 2023. P. 3–11. https://doi.org/10.1021/acsnano.9b06394.
25. Li Z., Wu Y. 2D early transition metal carbides (MXenes) for catalysis. *Small.* 2019. **15**. P. 1804736. https://doi.org/10.1002/smll.201804736.
26. Biswal L., Nayak S., Parida K. Recent progress on strategies for the preparation of 2D/2D MXene/gC_3N_4 nanocomposites for photocatalytic energy and environmental applications. *Cat. Sci. Tech.* 2021. **11**. P. 1222–1248. https://doi.org/10.1039/D0CY02156C.
27. Xie X., Zhang N. Positioning MXenes in the photocatalysis landscape: competitiveness, challenges, and future perspectives. *Adv. Funct. Mater.* 2020. **30**. P. 2002528. https://doi.org/10.1002/adfm.202002528.
28. Wang W., Hood Z.D., Zhang X. *et al*. Construction of 2D $BiVO_4$-CdS-$Ti_3C_2T_x$ heterostructures for enhanced photo-redox activities. *ChemCatChem.* 2020. **12**. P. 3496–3503. https://doi.org/10.1002/cctc.202000448.
29. Li J-Y., Li Y-H., Zhang F. *et al*. Visible-light-driven integrated organic synthesis and hydrogen evolution over 1D/2D CdS-$Ti_3C_2T_x$ MXene composites. *Appl. Cat. B: Environ.* 2020. **269**. P. 118783. https://doi.org/10.1016/j.apcatb.2020.118783.
30. Chen W., Han B., Xie Y. *et al*. Ultrathin Co-Co LDHs nanosheets assembled vertically on MXene: 3D nanoarrays for boosted visible-light-driven CO_2 reduction. *Chem. Eng. J.* 2020. **391**. P. 123519. https://doi.org/10.1016/j.cej.2019.123519.
31. Anasori B., Lukatskaya M.R., Gogotsi Y. 2D metal carbides and nitrides (MXenes) for energy storage. In: *MXenes.* Jenny Stanford Publ. 2023. P. 677–722.
32. Li M., Lu J., Luo K. *et al*. Element replacement approach by reaction with Lewis acidic molten salts to synthesize nanolaminated MAX phases and MXenes. *J. Am. Chem. Soc.* 2019. **141**. P. 4730–4737. https://doi.org/10.1021/jacs.9b00574.
33. Xu C., Wang L., Liu Z. *et al*. Large-area high-quality 2D ultrathin Mo_2C superconducting crystals. *Nat. Mater.* 2015. **14**. P. 1135–1141. https://doi.org/10.1038/nmat4374.
34. Geng D., Zhao X., Chen Z. *et al*. Direct synthesis of large-area 2D Mo_2C on in situ grown graphene. *Adv. Mater.* 2017. **29**. P. 1700072. https://doi.org/10.1002/adma.201700072.
35. Dehn W.M., McBride L. Studies of the chromoisomerism of Methyl Orange. *J. Am. Chem. Soc.* 1917. **39**. P. 1348–1377. https://doi.org/10.1021/ja02252a008.
36. Lü X-F., Ma H-R., Zhang Q. *et al.* Degradation of methyl orange by UV, O_3 and UV/O_3 systems: analysis of the degradation effects and mineralization mechanism. *Res. Chem. Intermed.* 2013. **39**. P. 4189–4203. https://doi.org/10.1007/s11164-012-0935-9.
37. Karri R.R., Tanzifi M., Yaraki M.T., Sahu J.N. Optimization and modeling of methyl orange adsorption onto polyaniline nano-adsorbent through response surface methodology and differential evolution embedded neural network. *J. Environ. Manag.* 2018. **223**. P. 517–529. https://doi.org/10.1016/j.jenvman.2018.06.027.
38. Peng C., Wang H., Yu H., Peng F. (111) TiO_{2-x}/Ti_3C_2: Synergy of active facets, interfacial charge transfer and Ti^{3+} doping for enhance photocatalytic activity. *Mater. Res. Bull.* 2017. **89**. P. 16–25. https://doi.org/10.1016/j.materresbull.2016.12.049.
39. Peng C., Yang X., Li Y. *et al*. Hybrids of two-dimensional Ti_3C_2 and TiO_2 exposing {001} facets toward enhanced photocatalytic activity. *ACS Appl. Mater. Interfaces.* 2016. **8**. P. 6051–6060. https://doi.org/10.1021/acsami.5b11973.
40. Jiang D., Sun X., Wu X. *et al*. MXene-Ti_3C_2 assisted one-step synthesis of carbon-supported TiO_2/Bi_4NbO_8Cl heterostructures for enhanced photocatalytic water decontamination. *Nanophotonics.* 2020. **9**. P. 2077–2088. https://doi.org/10.1515/nanoph-2020-0088.
41. Chen J., Zheng H., Zhao Y. *et al*. Preparation of facet exposed $TiO_2/Ti_3C_2T_x$ composites with enhanced photocatalytic activity. *J. Phys. Chem. Sol.* 2020. **145**. P. 109565. https://doi.org/10.1016/j.jpcs.2020.109565.

42. Steensma DP. "Congo" red: out of Africa? *Arch. Pathol. Lab. Med.* 2001. **125**. P. 250–252. https://doi.org/10.5858/2001-125-0250-CR.
43. Zahir A., Aslam Z., Kamal M.S. *et al*. Development of novel cross-linked chitosan for the removal of anionic Congo red dye. *J. Mol. Liq.* 2017. **244**. P. 211–218. https://doi.org/10.1016/j.molliq.2017.09.006.
44. Iqbal M.A., Ali S.I., Amin F. *et al*. La- and Mn-codoped Bismuth Ferrite/Ti_3C_2 MXene composites for efficient photocatalytic degradation of Congo Red dye. *ACS Omega.* 2019. **4**. P. 8661–8668. https://doi.org/10.1021/acsomega.9b00493.
45. Iqbal M.A., Tariq A., Zaheer A. *et al.* Ti_3C_2-MXene/bismuth ferrite nanohybrids for efficient degradation of organic dyes and colorless pollutants. *ACS Omega.* 2019. **4**. P. 20530–20539. https://doi.org/10.1021/acsomega.9b02359.
46. Sajid M.M., Khan S.B., Javed Y. *et al*. Bismuth vanadate/MXene ($BiVO_4/Ti_3C_2$) heterojunction composite: enhanced interfacial control charge transfer for highly efficient visible light photocatalytic activity. *Environ. Sci. Poll. Res.* 2021. **28**. P. 35911–35923. https://doi.org/10.1007/s11356-021-13315-9.
47. Brantom PG. Review the toxicology of a number of dyes illegally present in food in the EU. *EFSA J.* 2005. **263**. P. 1–71. https://doi.org/10.2903/j.efsa.2005.263.
48. Lu Q., Gao W., Du J. *et al*. Discovery of environmental rhodamine B contamination in paprika during the vegetation process. *J. Agric. Food Chem.* 2012. **60**. P. 4773–4778. https://doi.org/10.1021/jf300067z.
49. Imam S.S., Babamale H.F. A short review on the removal of rhodamine B dye using agricultural waste-based adsorbents. *Asian J. Chem. Sci* 2020. **7**. P. 25–37. https://doi.org/10.9734/ajocs/2020/v7i119013.
50. Wu Z., Liang Y., Yuan X. *et al.* MXene Ti_3C_2 derived Z–scheme photocatalyst of graphene layers anchored TiO_2/g-C_3N_4 for visible light photocatalytic degradation of refractory organic pollutants. *Chem. Eng. J.* 2020. **394**. P. 124921. https://doi.org/10.1016/j.cej.2020.124921.
51. Cui C., Guo R., Xiao H. *et al*. Bi_2WO_6/Nb_2CT_x MXene hybrid nanosheets with enhanced visible-light-driven photocatalytic activity for organic pollutants degradation. *Appl. Surf. Sci.* 2020. **505**. P. 144595. https://doi.org/10.1016/j.apsusc.2019.144595.
52. Ding X., Li Y., Li C. *et al*. 2D visible-light-driven TiO_2@Ti_3C_2/g-C_3N_4 ternary heterostructure for high photocatalytic activity. *J. Mat. Sci.* 2019. **54**. P. 9385–9396. https://doi.org/10.1007/s10853-018-03289-4.
53. Tran N.M., Ta Q.T.H., Noh J-S. Unusual synthesis of safflower-shaped TiO_2/Ti_3C_2 heterostructures initiated from two-dimensional Ti_3C_2 MXene. *Appl. Surf. Sci.* 2021. **538**. P. 148023. https://doi.org/10.1016/j.apsusc.2020.148023.
54. Diao Y., Yan M., Li X. *et al*. In-situ grown of g-$C_3N_4/Ti_3C_2/TiO_2$ nanotube arrays on Ti meshes for efficient degradation of organic pollutants under visible light irradiation. *Colloids. Surf. A: Physicochem. Eng.* 2020. **594**. P. 124511. https://doi.org/10.1016/j.colsurfa.2020.124511.
55. Howland M.A. Methylene blue. In: *History of Modern Clinical Toxicology.* Elsevier, 2022. P. 231–241.
56. Ramsay R.R., Dunford C., Gillman P. Methylene blue and serotonin toxicity: inhibition of monoamine oxidase A (MAO A) confirms a theoretical prediction. *Br. J. Pharmacol.* 2007. **152**. P. 946–951. https://doi.org/10.1038/sj.bjp.0707430.
57. Qu J., Teng D., Zhang X. *et al*. Preparation and regulation of two-dimensional $Ti_3C_2T_x$ MXene for enhanced adsorption-photocatalytic degradation of organic dyes in wastewater. *Ceram. Int.* 2022. **48**. P. 14451–14459. https://doi.org/10.1016/j.ceramint.2022.01.338.
58. Nasri M.S.I, Samsudin M.F.R, Tahir A.A. *et al*. Effect of MXene loaded on g-C_3N_4 photocatalyst for the photocatalytic degradation of methylene blue. *Energies.* 2022. **15**. P. 955. https://doi.org/10.3390/en15030955.
59. Liu T., Li L., Geng X. *et al*. Heterostructured MXene-derived oxides as superior photocatalysts for MB degradation. *J. Alloys Compd.* 2022. **919**. P. 165629. https://doi.org/10.1016/j.jallcom.2022.165629.

Authors and CV

Jamil A. Buledi, PhD in Analytical Chemistry from the National Centre of Excellence in Analytical Chemistry, University of Sindh, Pakistan in 2024. His research focuses on two-dimensional graphene-based electrochemical sensors. He started his career in 2018 as a research associate and completed three projects funded by HEC Pakistan. His expertise includes 2D nanocomposites, metal nanoclusters, hybrid nanocomposites, sensors, degradation and removal of organic pollutants. Authored over 60 research and review articles and book chapters, obtaining an H-index of 23. E-mail: kjamil234@gmail.com, https://orcid.org/0000-0002-9424-2945

Sergii Golovynskyi defended his Ph.D. thesis in Physics and Mathematics (Optics, Laser Physics) in 2012 at the Taras Shevchenko National University of Kyiv. In 2012, he started his research career at the V. Lashkaryov Institute of Semiconductor Physics, NASU. Since 2016, he is associate researcher at Shenzhen University, China. His main research activity is in the fields of semiconductor physics and optics, spectroscopy, nanomaterials, and optoelectronics. Author of more than 80 scientific articles, obtaining an H-index of 22. He serves on the editorial board of several journals. E-mail: serge@szu.edu.cn, https://orcid.org/0000-0002-1864-976X

Vladyslav Kravchenko defended his PhD thesis in Physics and Mathematics (Optics and Laser Physics) in 2000 at the Taras Shevchenko National University of Kyiv. He is an associate professor at the Faculty of Physics of the same university. Author of over 100 scientific publications, and 6 textbooks. The area of his scientific interests includes the optics of semiconductors and biophotonics.
E-mail: kravm@knu.ua,
https://orcid.org/0009-0001-1315-416X

Junle Qu, PhD in Physical Electronics from the Xi'an Institute of Optics and Precision Mechanics, Chinese Academy of Sciences in 1998, Chair Professor of Optical Engineering at Shenzhen University, China. His research interests include optoelectronics, nanomaterials, nonlinear optical microscopy, fluorescence imaging, superresolution optical imaging, and their applications in biomedicine. Authored over 700 scientific papers and over 90 issued patents, obtaining an H-index of 76. He is a senior member of SPIE and the Chinese Optical Society and an editor of several journals. E-mail: jlqu@szu.edu.cn,
https://orcid.org/0000-0001-7833-4711

Iuliia Golovynska, PhD in biology from the Institute of Biology and Medicine, Taras Shevchenko National University of Kyiv, Ukraine in 2011, then worked there as a junior researcher. Since 2016, she is an associate researcher at the Shenzhen University, China. She works on photochemistry, organic dyes, nanomaterials, biophotonics, biomedical imaging, photobiomodulation and therapy. Author of 36 scientific articles, obtaining an H-index of 16.
https://orcid.org/0000-0003-3916-6588

Amber R. Solangi, distinguished professor in analytical chemistry, PhD (2007) from the National Centre of Excellence in Analytical Chemistry (NCEAC), University of Sindh, Pakistan. In 2010, she completed her postdoctoral research at the School of Chemistry, Monash University, Australia. She is Full Professor, since 2017 serves as the Director of NCEAC, University of Sindh. She has secured and completed 4 research projects. With over 140 published research and review articles, she has earned 3000+ citations with an H-index of 34. https://orcid.org/0000-0002-3852-1245, E-mail: amber.solangi@usindh.edu.pk, ambersolangi@gmail.com

Authors' contributions

Buledi J.A.: conceptualization, formal analysis, writing original draft, visualization, writing – review & editing.
Golovynskyi S.: conceptualization, formal analysis, visualization, writing – review & editing.
Kravchenko V.M.: writing – review & editing.
Qu J.: resources, supervision, writing – review & editing.
Golovynska I.: formal analysis, writing – review & editing.
Solangi A.R.: conceptualization, formal analysis, drafting, writing – review & editing.

Двовимірні фотокаталізатори з інтегрованими максенами: новий рубіж у сталій деградації органічних барвників

J.A. Buledi, S. Golovynskyi, В.М. Кравченко, J. Qu, I. Golovynska, A.R. Solangi

Анотація. Двовимірні (2D) композити на основі максенів, клас графеноподібних карбідів та нітридів перехідних металів, є чудовими матеріалами для фотокаталітичного застосування завдяки своїм перспективним характеристикам, таким як налаштовувані функціональні можливості та велика площа поверхні. Для виготовлення фотокаталізаторів на основі максенів використовуються різні шляхи синтезу, а саме: гідротермальний, сольвотермічний, електростатична самозбірка та хімічне осадження з парової фази. Сольвотермічні та гідротермальні методи синтезу підвищують кристалічність та прискорюють перенесення заряду, запобігаючи рекомбінації та підвищуючи фотокаталітичну активність. Крім того, методи травлення впливають на фізико-хімічні властивості максенів, змінюючи ефективність видалення забруднюючих речовин. Композити максенів використовуються як перспективні фотокаталізатори для деградації органічних барвників, включаючи конго червоний, метиленовий оранжевий, родамін В та метиленовий синій. Такі композити максенів, як TiO_2/Ti_3C_2, Bi_2WO_6/Nb_2CT_x та MXene/g-C_3N_4, демонструють чудову фотокаталітичну ефективність, досягаючи швидкості деградації понад 90% під впливом видимого світла. Однак, такі проблеми, як масштабованість, енергоспоживання та структурна стабільність, потребують подальшого дослідження для оптимізації їхнього великомасштабного застосування.

Ключові слова: композити максенів, 2D нанокомпозити, відновлення навколишнього середовища, органічні забруднювачі, забруднення навколишнього середовища.